Electron-Beam Generated E×B Plasma for Air-Breathing Propulsion- a concept study

IEPC-2022- 443

Presented at the 37th International Electric Propulsion Conference
Massachusetts Institute of Technology, Cambridge, MA USA
June 19-23, 2022

Yevgeny Raitses,[1] Nirbhav Chopra,[2] and Jacob Simmonds[3]
Princeton Plasma Physics Laboratory, Princeton University, Princeton, NJ 08543, USA

We analyze the feasibility of airbreathing plasma propulsion with limited compression. Ionization of neutrals is performed by electron beams. Key challenges include: 1) high power requirements to generate the beams, 2) effective trapping of beam electrons to maximize their efficient use for ionization of the incoming air, and 3) suppression of beam plasma instabilities. There are also critical technical and materials challenges which are not considered in this paper.

I. Introduction

A need exists for spacecraft to occupy a very low orbit: somewhere near the bottom of the thermosphere (i.e., at just above the mesosphere, altitudes of 100 – 200 km).[1,2] The challenge is largely in overcoming drag as the air densities are not insignificant. To compensate the air drag, the on-board propulsion should generate thrust, T, equal to the total drag force, F_D, on the spacecraft, including but not limited to the front surface facing the incoming air, F_{front}, and side surfaces (so-called skin drag), F_{sk}:

$$T = \sum F_{Drag} \approx F_{front} + F_{sk} \, . \tag{1}$$

If it is desired for this spacecraft to be parked in this orbit indefinitely, then it would require that the propellant be harvested from the surrounding atmosphere, which exists at very low pressures 10^{-6} – 10^{-4} Torr for relevant altitudes. An inlet scoop (Fig. 1) is one of the practical designs for such a concept that provides typical gas pressure conditions suitable for ionization.[3,4] Indeed, such an air-breathing collector has been investigated by the European Space Agency (ESA) to collect air for use in an electric thruster.[2,5] The ambient air is compressed to pressures (~ 0.1 mTorr) at which the air can be ionized under typical operating conditions of conventional ion and Hall thrusters, the latter of which is an E×B space propulsion device.[6] The ESA concept was designed for flight at 200 km, and in a recent press release demonstrated the operation of the concept when servicing a Hall thruster.[7] For lower altitudes, the main drawback of this approach would be the enhanced input electric power requirement associated with the use of inlet compression. This requirement implies that the satellite must operate at high altitudes where the available on-board power is sufficient to power the plasma thruster enough to compensate the drag.

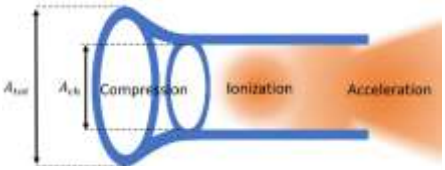

Figure 1: Schematic of orbiting spacecraft model to estimate requirements for ultra-low-Earth orbit parking.

An alternative concept of airbreathing plasma propulsion was proposed by Pekker and Keidar.[8] Compared to the ESA thruster, their airbreathing plasma propulsion uses a simpler flow-through configuration, in which the

[1] Principal Research Physicist, Plasma Science & Technology, yraitses@pppl.gov.
[2] Graduate Student, Graduate Program in Plasma Physics, Department of Astrophysical Sciences, nschopra@pppl.gov.
[3] PhD Candidate, Mechanical and Aerospace Engineering, jsimmond@pppl.gov. Current position and affiliation: Technologist, NASA Jet Propulsion Laboratory, respectively.

incoming airflow is ionized and accelerated directly in the annular channel of the Hall thruster, without preliminary compression. For the considered orbits of this satellite at 90-95 km, the neutral density is presumably large enough ($> 10^{13}$ cm^{-3}) to allow efficient ionization of the incoming airflow. Yet, the power needed to propel this satellite at such altitudes is rather large ~ 0.7-0.8 MW.[8] Moreover, because this hypothetical airbreathing Hall thruster uses an annular geometry, it will experience more drag due to the inner cylinder with inner magnet at the center of the annular channel, which was not accounted in the model of Ref. 8. This annular geometry is needed for the implementation of a conventional Hall thruster magnetic field with a strong radial magnetic field in the gap between the inner and the outer channel walls.[8]

In this work, similarly to Ref. 8, we also consider an airbreathing ExB plasma propulsion scheme without the inlet compression or with an insignificant compression of $\kappa \equiv \frac{A_{tot}}{A_{ch}} \leq 5$, where $A_{tot} = \pi R^2$ is the total area of the cylindrical geometry thruster/satellite facing the incoming air flow, R is the outer radius of the satellite, and A_{ch} is the area of the flow-through channel. We use here the so-called cylindrical Hall thruster (CHT) configuration.[9] Unlike the annular geometry Hall thruster, the CHT configuration does not have the inner channel, and therefore its open-channel airbreathing implementation should experience a smaller drag from the incoming air. Electron beam (e-beam) ionization of the incoming air is considered as it is the most efficient way of gas ionization in terms of the ion cost per electron-ion pair created.[10] For example, for the ionization of air, the electron beam can provide the lowest ionization cost of $w_i^{min} \approx 34$ eV.

For our simplified analysis, we consider an idealized situation when the satellite with an airbreathing thruster does not carry any on-board propellant to initiate/sustain the plasma operation. Therefore, both thruster electrodes operate in air. Moreover, in this analysis on-board power requirements are only limited to the ion acceleration and do not account for the power needed to generate and sustain electron beams. Similarly, to Pekker and Keidar's suggestion, the assumption is that these beams can be generated from another satellite flying at higher orbits where the air drag force is negligible.[8] Satellites carrying electron beam generating systems (e.g. compact linear accelerators) at high altitudes and lunching relativistic electron beams to lower altitudes have been considered for studies of electric discharges in the mesosphere[11] and mapping magnetospheric field lines[12] etc. For an air breathing plasma propulsion application, no relativistic beams are required. There are early works on spaceborne launching of lower energy electron beams (< 10 keV).[13] We recognize that there are fundamental and technical challenges with launching such low energy electron beams from satellites (e.g., satellite charging, beam instabilities). However, these considerations for the external electron beam generation are out of scope of this paper. We note, however, that if it would be affordable for the on-board power source to support the electron beam generation in this airbreathing thruster (e.g., solar panel configurations with minimal contribution to the air drag, or reduced e-beam power requirement at high altitudes), there would be no need for the external source of the electron beams.

This paper is organized as follows. In section II, we present a simplified analysis of the effect of compression on the thruster power and specific impulse requirements. Section III deals with the ionization by electron beams. In section IV, we make important remarks on beam stability for the considered conditions.

II. Effect of the compression on thruster performance

We consider a cylindrical satellite of the radius, R, and the length, L , propelled by an open channel airbreathing plasma propulsion configuration (Fig. 1). For this satellite, the drag forces in Eq. (1) are given by

$$F_{front} = \rho_{amb} v_o^2 A_{tot} \left(1 - \frac{1}{\kappa}\right) \tag{2}$$

$$F_{sk} = C_{sk} 2\pi R L \rho_{amb} v_o^2 \tag{3}$$

Therefore, the total thrust required to compensate the aerodynamic drag can be expressed as

$$T = \rho_{amb} v_o^2 A_{tot} \left(1 - \frac{1}{\kappa}\right) + C_{sk} 2\pi R L \rho_{amb} v_o^2. \tag{4}$$

Here, ρ_{amb} is the mass density of the ambient air, $v_o \approx 7.8\ km/s$ is the orbital velocity of the considered satellite and A_{tot} is the total frontal area of the satellite. For the skin drag (second term in the brackets), C_{sk}, is aerodynamic skin drag coefficient. Assuming a diffusive reflection of gas molecules from the satellite front wall,[8] and using Eqs. (1) and (2), the required input electric power, P_{req}, can be estimated for a given thruster efficiency, η_T, which is the ratio of the thrust power required for the drag compensation (Eq. 1) to the electric power:

$$P_{req} = \frac{T^2}{2\dot{m}_i \eta_T} = \frac{\left[F_{front} + F_{sk}\right]^2}{2\dot{m}\, \eta_{ion} \eta_P}, \tag{5}$$

where $\dot{m}_i = \rho_{amb} v_o A_{tot}\, \eta_P$ is the ion mass flow rate, which is the ionized fraction of the incoming air flow, $\dot{m} = \rho_{amb} v_o A_{tot}$. For the sake of this simplified analysis, we expressed here the thruster efficiency as $\eta_{ion}\eta_P$ where $\eta_{ion} \equiv I_{ion} V_{ion}/P_{req}$ is the ion acceleration efficiency, and the propellant utilization efficiency, $\eta_P \equiv \dot{m}_i/\dot{m} = eMI_{ion}/\dot{m}$. $I_{ion}$is the current of the ions acquiring the energy eV_{ion} to generate the thrust, e is the electron charge and M is the atom mass. The propellant utilization is estimated using an analytical expression obtained from a simplified quasi one-dimensional model of the plasma flow in a cylindrical channel.[9] This model accounts for effective ion wall losses ~ R/L . Moreover, Eqs. (2), (4), and (5) account for the compression which characterizes an increase of the density of the incoming flow inside the thruster channel.

In this work, we are focused on the conceptual analysis of ionization by the electron beams, but for simplicity, all our estimations are made for N_2 ionization with the flow velocity of N_2 equal to the orbital velocity, v_o, for relevant altitudes. We do acknowledge that a chemical composition of the upper atmosphere at the altitudes considered here is more complex and includes a significant fraction of atomic oxygen. The ionization cost of atomic oxygen is lower than the ionization of the molecular nitrogen.[14] Therefore, there may be a substantial fraction of lighter oxygen ions participating in the thrust generation. In addition, the formation of negative oxygen ions can change the plasma composition and properties. All these factors will change with the altitude as the chemical composition changes too. Therefore, a more complex analysis is required to account for these changes. Here, our analysis is limited to electron-impact ionization of nitrogen molecules: $e + N_2 \rightarrow 2e + N_2^+$, by high energy beam electrons (~ 0.1-1 keV).[15] Thus, we did not consider ionization by non-thermal energetic electrons generated by beam-plasma interactions and heating of secondary electrons resulting from the air ionization.

Fig. 2 illustrates results of the analysis for a hypothetical airbreathing plasma thruster integrated into the satellite at the altitude of 170 km. Here, we considered a conservative case of a power-limited satellite with the power estimated using Eq. (5). The available power is for the ion acceleration. The external surface of this hypothetical satellite-thruster (Fig. 1) is covered with solar panel arrays to power the thruster, where at most, sunlight is exposed to a rectangular area. This consideration implies that there are no solar panels extended beyond the satellite outer radius and length. Thus, the available solar power is also a function of the satellite/thruster dimensions: $P_{solar} = 2RLW_{solar}\eta_{solar}$, where L is the satellite length, $W_{solar} = 1361$ W/m^2 is the solar flux at Earth, and $\eta_{solar} = 0.25$, the assumed efficiency of the solar panel array. The operation of this satellite is limited to the following design condition:

$$P_{req} \leq P_{solar}. \tag{6}$$

Note that the solar angle of incidence over the orbit is heavily dependent on the orbit chosen, with optimal conditions found in solar-synchronous orbits. Our analysis here assumes such optimal conditions, where a scaling factor on solar power could be applied, changing with orbital requirements. Other assumptions are as follows. The thruster efficiency was assumed to be constant, $\eta_T \approx 0.1$ that is comparable, but smaller than the thruster efficiency measured for a laboratory Hall thruster operating with nitrogen gas.[16] A relatively low efficiency of this laboratory thruster is at least partially due to power losses on excitation and ionization of the nitrogen.

Fig. 2 shows results of estimations for the required power (Eq. (5) and *Isp*, for two satellite cases: short (L = 1 m) and long (L = 3 m) satellites, with the same total frontal area, $A_{tot} \approx 0.5$ m^2, and for two different levels of the available power. Here, we define an ion specific impulse for the condition when the thrust balances the air drag, Eq. (1),

$$Isp \equiv T/\dot{m}_{ion} g \approx \frac{T}{\eta_P \dot{m} g} = \frac{1}{g} \frac{\left(\rho_{amb} v_o^2 A_{tot}\left(1-\frac{1}{\kappa}\right) + C_{sk} 2\pi RL \rho v_o^2\right)}{\eta_P \rho_{amb} v_o A_{tot}}, \tag{7}$$

where g is the gravitational acceleration. In this formulation, the thrust is generated only by ions i.e., acceleration of neutral species in the thruster or charge exchange between ions and neutrals are neglected.

In addition, for the longer satellite of L = 3 m, in order to show a relative effect of the skin drag, which is currently undefined for the altitudes considered in this work, two skin drag coefficients were compared: C_{sk} = 0 and 0.01 (Fig. 2). An estimate for C_{sk} was made by using Prandtl's one-seventh-power law, $C_{sk} = 0.027/Re_x^{1/7}$, where $Re_x = \rho_{amb} v_o x/\mu$ is the Reynolds number calculated at the center of a pipe of length L ($x = L/2$), and μ is the dynamic viscosity of air. A conservative value of μ was taken to be $\mu = 1.32 \times 10^{-5}$ N s m^{-2}, the dynamic viscosity of the atmosphere at 80 km altitude above the sea level. The total frontal area of the satellite is taken to be $A_{tot} \approx 0.5$ m^2.

For each considered satellite length case, Figure 2a shows the dashed horizontal lines which correspond to the solar power limit available for the ion acceleration. All required power levels below these lines can be considered feasible for a power-limited satellite. In Fig. 2b, the vertical dashed lines show the limiting compression factors for each length and skin drag case, corresponding by color. The intersections of Isp vs κ curves with these dashed lines of the same

define the feasible operational envelop for the power-limited satellites. All values of the compression factor from the left side of the intersections can be considered as feasible for this power-limited satellite. For the second satellite case with $L = 3$ m and $C_{sk} = 0$, the condition Eq. (6) fulfilled for the full range of the compression factor shown in Fig. 2a. Therefore there is no vertical dashed line on Fig. 2b for this case. If we would not limit the available power by the satellite surface area covered with solar panels or use an alternative power source of larger power density, then all regimes and compression factors shown in Fig. 2 could be feasible.

Complex trends in the dependences shown in Fig. 2 are governed by a tradeoff between power requirements to compensate the air drag which increases with the compression factor, and the ionization efficiency which also increases with the compression factor. At small compressions, the drag is small and so the required power is small. At larger compressions, more power and Isp are required to compensate the increased drag. At some point, the increase of the propellant utilization at elevated gas pressures (larger compression and neutral densities) gets stronger than the increase of the drag due to the compression. This explains, for example, the presence of the maximum on the *Isp* curve (Fig. 2b). Despite these advantages in propellant utilization, the power requirements of high compression are a few times larger than the low compression case.

For the considered altitude of 170km, in order to leverage the advantages of low compression (the left side of the dashed line in Fig. 2) the air plasma thruster needs to operate with *Isp* of 200-1400 s (Fig.2b). From the energy conservation for the ion accelerating by the electric field, the ion exhaust velocity is

$$v_i = \sqrt{\frac{2eV_{ion}}{M} + v_0^2}. \tag{8}$$

In the frame of the satellite, the thruster is accelerating an already-moving flow, and hence the ion velocity at the exit is related to the specific impulse as define in Eq. (7) as $v_i = gIsp - v_o$. Then, the necessary voltage to achieve the required Isp can be expressed as

$$V_{ion} = \frac{M}{2e}(gIsp)^2\left(1 + \frac{2v_0}{g\,Isp}\right). \tag{9}$$

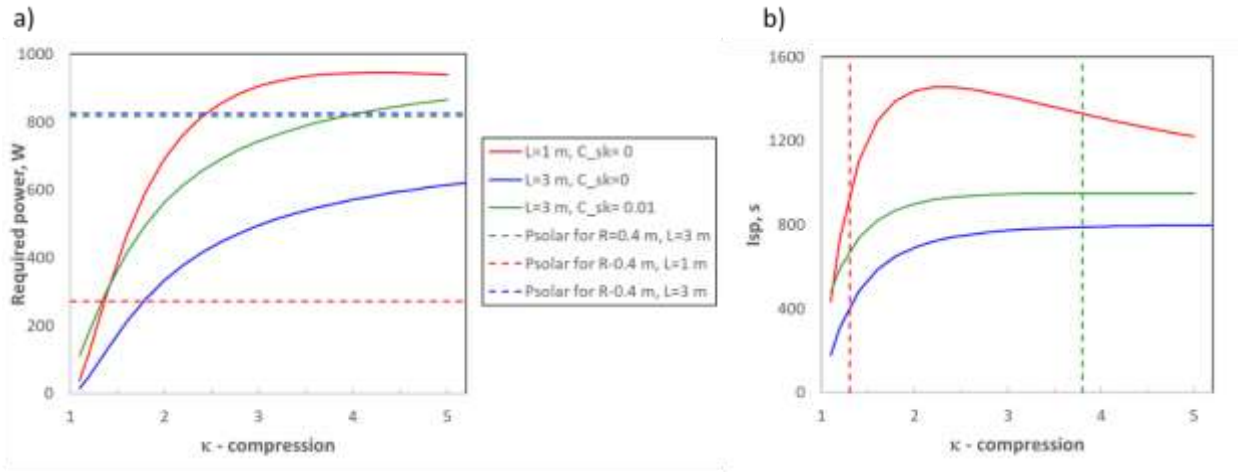

Figure 2: Effect of the compression factor on a) the required input electric power (Eq. (4)) and b) *Isp* requirements to generate the thrust for drag compensation of two power-limited satellites with open channel airbreathing plasma propulsion (Fig. 1) with the same radius of 0.4 m and two different lengths of 1 m and 3 m, respectively, at the altitude of 170 km. For a shorter satellite of $L = 1$ m the skin drag coefficients is taken to be C_{sk} =0. For the longer satellite of $L = 3$ m, two cases are considered C_{sk} =0 and 0.01. The total efficiency is taken as 10%. We assumed the electron beam energy to be 1 keV. Note that at the compression factor κ =1, there is no air drag as there are no walls interacting with the air. In Fig. 2a, the horizontal lines show the available solar power for given length of the thruster. In Fig.2b, the intersections of dashed and solid lines of the same colors correspond to the threshold compression at which the required power is equal to the available solar electric power.

Fig. 3 shows the acceleration voltage required to achieve Isp, for the first satellite case of Fig. 2 (L = 1 m, C_{sk} = 0). Two electron beam energy cases are considered: 0.2 and 1 keV. In general, the voltage behavior repeats the Isp of Fig. 2a. The existence of the maximum voltage has also the same reason as it was explained above for the Isp dependence on the compression.

Note that the required accelerating voltage is less than 70 V, which is much lower than the voltage range in which conventional Hall thrusters operate ($\geq 10^2$ V). However, in these thrusters, the input power supports both acceleration and ionization processes. In the airbreathing thruster considered here, the ionization is by electron beams which are generated by an external source. In this regard, this airbreathing plasma propulsion is more like a two-stage Hall thruster approach in which the ionization and acceleration can be controlled separately.[17],[18] The two-stage concept was previously proposed for airbreathing Hall thrusters, including the two-stage cylindrical Hall thruster with the ionization stage using electron cyclotron resonance (ECR) heating. The concept used a high compression of the incoming air (factor 500) to sustain high ionization in the ECR stage.[6] From our analysis of the compression effect on the required power (Eq. 4), such a high compression factor does not seem to be practical.

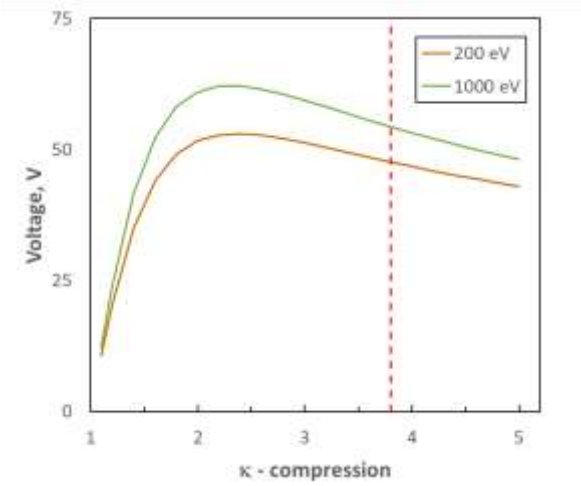

Figure 3: The acceleration voltage of the airbreathing plasma thruster required to achieve *Isp* for the satellite case with L=1 m and Csk = 0 at the altitude of 170 km. Two electron beam energy cases are considered: 0.2 and 1 keV, respectively. The vertical dashed line is the same as the line of Fig. 2b for the corresponding case (the first case).

Note that a two-stage plasma thruster concept is commonly used for gridded ion thrusters and may be applicable for the airbreathing application as well. There are however many issues and unknown factors associated with the use of gridded thrusters at the relevant altitudes between 100 and 200 km including, but not limited to, grid chemical erosion by oxygen atoms, space charge limitation on the thrust density at low voltages required for the targeted Isp range etc.

III. e-Beam ionization at low pressures

The ionization of air by high energy electrons (10^2-10^3 eV) forming electron beams at low pressures can be beneficial to achieve the minimum ionization cost per created electron-ion pair.[10] Following modeling results of Ref. 14 for molecules present in air (e.g., N_2, O_2), the ionization cost reaches its lowest values at electron energies of ε_b ~200-300. The model included all inelastic processes occurring at the impact of electron on the molecule (e.g., excitations, ionization). For each atomic and molecular species, this energy is higher than the ionization potential precisely because it accounts for excitation of atoms and molecules.[14] The saturation at electron energies above 300 eV is due to losses on excitation and the reduction of the ionization cross-sectional area. These modeling results were verified in simulations and confirmed in experiments. Thus, for the ionization cost of $w_i^{min} \approx$ 36 eV (for N_2), electrons with energies of 200-300 eV may have 5-7 ionizing collisions before they lose the energy needed for ionization of N_2 molecules by a direct impact ionization. For high energies of $\varepsilon_{beam} \geq 0.5$ keV, the energy relaxation length for the electron beam in N_2 gas can be estimated using the following semi-empirical formula which was validated in simulations and experiments:[19]

$$L_{R>500eV} \approx 1.1 \cdot 10^{21}\, \varepsilon_{beam}^{1.7}/N, \tag{10}$$

where ε_{beam} is the electron beam energy in kiloelectron volts and N is the neutral gas density in 1/cubic meters. The length is in meters. A more general formulation of the energy relaxation length for beam electrons is[20]:

$$L_R \approx \frac{\varepsilon_{beam}}{2(d\varepsilon_b/dz)}, \tag{11}$$

where $d\varepsilon_b/dz$ is the energy loss of beam electrons in z-direction due to elastic and inelastic scattering off neutrals. This loss can be estimated using the Bethe formula and data reference survey of Ref. 21 (for a given e-beam energy, neutral density was multiplied by the loss function). Both Eqs. (10) and (11) agree well at $\varepsilon_{beam} \geq 0.5$ keV.

Table 1 shows examples of the electron beam relaxation length estimated using Eqs. (10) and (11) for electron energy of 1 keV and 0.2 keV, respectively at an altitude of 90 km and 140 km. When the relaxation length is comparable with or less than the channel length, the beam electrons are more effectively used for ionization. For the altitude of 90 km and the electron beam energy of 200 eV, the relaxation length is comparable with the considered channel lengths (Fig. 2) and may be implemented in practice. For a 1keV beam at the same altitude and for the higher

altitude cases, the beam relaxation length is extremely long (Table 1). Trapping of high energy electrons inside the channel may help support effective ionization for such long relaxation lengths. This may be accomplished by guiding and confining the beams with applied magnetic field. For example, magnetic field cusps combined with biased electrodes can form a so-called magneto electrostatic trap. Such electron traps are used for example, in sputtering magnetrons,[22] cylindrical Hall thrusters,[9,23] wall-less Hall thruster[24] and HEMP thruster.[25] If the beams are effectively trapped inside the channel, we may roughly assume that $L_R \sim L$.

Table 1: Approximate values of the energy relaxation length [in meters] of beam electrons estimated using formulations of Refs. 19 and 20, for two different electron energies 0.2 keV and 1 keV and neutral densities at corresponding altitudes. The neutral density was estimated for the corresponding altitudes and the compression factor of 2.

Electron energy/Altitude	$L_R(\varepsilon = 0.2$ keV) (Eq. 11)	$L_R(\varepsilon = 1$ keV) (Eq. 10)
90 km	1.5	15
140 km	1.5×10^3	15×10^3

The plasma density which needs to be generated by the electron beam to provide the required thrust can be roughly estimated from the mass conservation of heavy species and energy conservation for ions accelerated by the electric field (Eq. (8)).[8] Then, using the above definition of the propellant utilization efficiency, the required ratio of the ion density after the ion acceleration region to the density of atoms at the inlet of the airbreathing thruster is

$$\gamma \equiv \frac{n_i}{n_a} = \eta_p \frac{v_0}{v_i}, \tag{12}$$

where n_a the density of incoming air and n_i the ion density in the accelerated ion flow. Figure 4 shows the density ratio estimated for the same cases as shown in Fig. 3. According to Eq. (12), if there are no ion losses along the ion accelerating region, the density ratio should be higher upstream of the ion acceleration region where ions are slower. When both densities are taken at the same location, the density ratio is close to a traditional definition of the ionization degree, $\frac{n_i(z)}{n_i(z)+n_a(z)}$. Thus, plots of Fig. 4 gives underestimated values of the minimum ionization degree required for the thruster.

Note that the trends for the density ratio and Isp (can be deduced from Fig. 2b, for the first case) are somewhat similar. Some differences (e.g., shift of the minimum ratio vs the maximum of the Isp (Fig. 2b)) are due to the dependence of the density ratio on the propellant utilization (Eq. 12) which also changes with the compression.

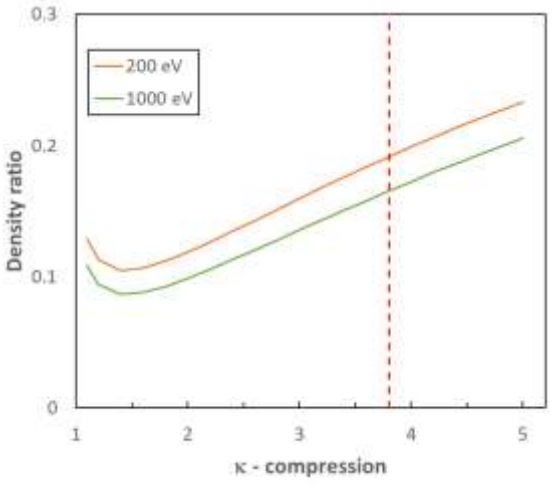

Figure 4: The ratio of the density of ions accelerated in the airbreathing plasma thruster to the density of neutrals at the thruster inlet for the same cases as shown in Fig. 3.

To determine the required beam current density, J_b,we consider a simplified balance between the ionization in the volume and plasma losses of the walls and plasma escape through the exit of the thruster channel.[8,20] The source term of volumetric ion production by the incident electron beam can be expressed as[20] $S \approx \frac{J_b}{e}\frac{1}{w_i}\frac{d\varepsilon_b}{dz}$. For the thruster cases with $L_R > L$, we make an assumption of the full trapping of energetic electrons from the beams i.e., $S \sim \frac{J_b}{e}\frac{1}{w_i}\frac{\varepsilon_b}{L}$. The wall losses are proportional to $\frac{\Gamma_w}{R_{ch}}$, where $\Gamma_w \approx 0.6 n_i v_B$ is the ion flux to the wall, n_i is the channel radius, n_i is the ion density in the channel, $v_B = \sqrt{T_e/M}$ is the Bohm velocity, and T_e is the electron temperature[9]. The factor of 0.6 accounts for the plasma density drop in the pre-sheath near the wall, which we assume to be planar. The plasma loss rate due to plasma escaping through the thruster exit is given by $\frac{J_{ion}}{eL}$, where $J_{ion} = I_{ion}/A_{ch}$ is the ion current density. The corresponding rate balance equation is $S\pi R^2 L = \frac{J_w}{e} 2\pi RL + \frac{J_{ion}}{e}\pi R^2$. Then, from the above balance between ionization wall loss, and ion escape loss, the required current density can be expressed as

$$J_b = 2J_w \frac{w_i(\varepsilon_b)L}{\varepsilon_b R}\left(1 + \frac{J_i}{J_w}\frac{R}{2L}\right) \tag{13}$$

In Eq. (13), unlike the case considered in Ref. 20 with particles losses due to dissociative recombination, the dominant losses are on the channel wall and through the channel exit. We checked this statement and confirmed that the dissociative recombination time $\tau_{rec} \approx 1/\beta_{rec} n_a$ is much larger than a characteristic time of ion wall losses, R/v_B or R^2/D_a and even more so for the transient time of the ions escaping through the channel exit, R/v_i. Here, D_a is the coefficient of ambipolar diffusion.[26] Table 2 lists examples of the required current densities to generate the plasma density in the airbreathing thrusters. The estimates are for the same parameters as listed in Table. 1.

Note that the current densities listed in Table 2 can be achieved using either cold cathodes emitting electrons due to ion-induced secondary electron emission (for the 140 and 180 km cases) or by thermionic cathodes (~ 1 A/ cm^2, e.g., for 90 km cases). For higher current densities, it may require the use of plasma cathodes to generate the beam that will have to be implemented either by carrying inert gas propellant on board of the satellite or using a compression stage to supply the air.

Table 2: Approximate values of the electron beam current density and the beam power required to generate the plasma density for parameters of Fig. 4. The current density was estimated using Eq. (13) for the conditions listed in Table 1. The ionization cost $w_i(\varepsilon_b)$ was obtained for N_2 from Ref. 14.

Electron energy/Altitude	0.2 keV		1 keV	
	Current density A/cm^2	Beam power W	Current density A/cm^2	Beam power W
90 km	2.9	1.5×10^6	0.56	1.4×10^6
140 km	2.3×10^{-3}	1.2×10^3	3.96×10^{-4}	994
170 km	1.7×10^{-4}	83	2.47×10^{-5}	62

For the ionization of the incoming air, the electron beams must cover the whole volume of the thruster channel. Then, assuming that the beams can propagate along the channel, the total electron beam current is $I_b = J_b A_{ch}$, and the beam power, $P_b = I_b \varepsilon_b$. Table 2 includes rough estimate of the required beam power. For the lower altitude (90 km), the beam power is in MW range that is similar to Pekker and Keidar's results of Ref. 8. Compared to this beam power level, the available input power for the power-limited thruster considered here is only a negligible fraction. For the higher altitude (140 km), the beam power is in kW range that is still an order of magnitude higher than the available power for the considered satellite configuration (solar panels only on the external surface of the satellite). Even if this beam power would be available on board of satellite, the efficiency of this proposed system would be extremely low ~ 1%. Thus, even for low beam power regimes, the only seemingly viable option is also to launch these beams from another satellite orbiting at higher altitudes.

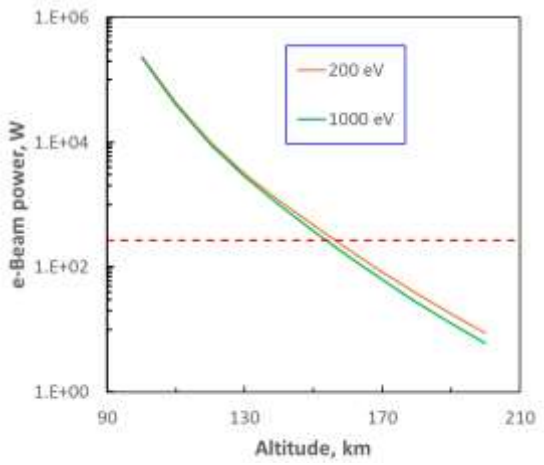

Figure 5: Electron beam power required to sustain the considered air-breathing plasma thruster as a function of the operating altitude. For simplicity of this analysis, we considered the e-beam ionization of N_2.

Note that for the considered power-limited airbreathing propulsion with electron beams of 0.2 keV and 1 keV, the required beam power gets smaller than the power limit of about 270 W at the altitudes above 170 km (Fig. 5). Recall that this artificially imposed limit is because of the restricted solar panel area limited by the satellite size. For example, at the altitude of 200 km, which was in the focus of ESA efforts on airbreathing Hall thruster[5], the required beam power is below 40 W that is about 13% of the available power on the board of our hypothetical thruster. Without the size-dependent power limit, the required beam power becomes less than the thruster power (Eq. (5) required to compensate the air drag starting even from lower altitudes (Fig. 6). In this plot, the dashed line corresponds to the case when the beam power equals thruster power. In principle, in the absence of the power limit described by Eq. (6), for e-beam power levels below this dashed line, the on-board electron beam source appear to be a reasonable option for consideration as such sources can be implemented in practice.

IV. Remarks on e-beam stability

A key challenge for the use of electron beams for the airbreathing plasma thruster at high altitudes is that it requires an efficient trapping of beam electrons inside the channel until they spend their available energy for ionization of the incoming air. At the altitudes of above 170 km, the beam relaxation length is much higher than the values shown in Table 1. For example, at the beam energy of 38 eV corresponding to the minimum ionization cost for N_2,[14] the energy relaxation length estimated using Eq. (10) is about 5 km. This implies that the beam should bounce back and forth thousands of times along and across a 1 m length x 1 m diameter thruster chamber in order to exhaust all its energy. Even if it is technically feasible to implement such a trap, these beams may be a subject to beam plasma and two-stream instabilities[20] as well as to a variety of electrostatic instabilities common to ExB plasmas[27] at low pressures (e.g., collisionless Simon-Hoh instability[28]). These instabilities may cause an energy spread and scattering of beam electrons, causing beam losses. The same instabilities may take place at altitudes lower than 170 km as well. To get an idea if electron beams in the airbreathing thruster are subject to beam plasma instability, we used the minimum stability criterion for a linear velocity spread:[20]

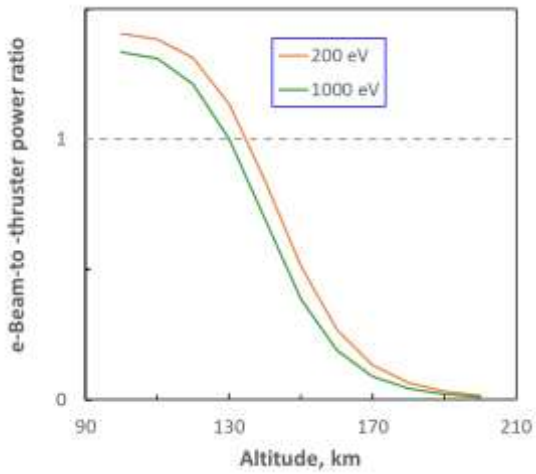

Figure 6: The e-beam power required to sustain the ionization to the thruster power required to compensate the air drag for the considered airbreathing thruster (Fig. 2, case 1). In this analysis, we considered the e-beam ionization of N_2.

$$\nu_{en} \geq 2\pi\omega_{pe}\frac{n_{be}}{n_{pe}}\left(\frac{v_{max}}{\Delta v}\right)^2, \tag{14}$$

where ν_{en} is the electron collision frequency, ω_{pe} is the electron plasma frequency, $n_{pe} \approx n_i$ is the density of plasma electrons, and n_{be} is the density of beam electrons, v_{max} is the maximum velocity of beam electrons, and Δv is the velocity spread. If $v_{max} \geq \Delta v$ e.g., $\frac{v_{max}}{\Delta v} \sim 1$, Eq. (14) is not satisfied almost for all considered conditions except at lower altitudes of 90-100 km where electron neutral collisions are significant enough to satisfy to the above stability condition. One of possibilities to prevent this instability is to increase the spread of the beam directed velocity, $\Delta v \geq v_{max}$.[20, 29] Analysis of this and other solutions is outside the scope of this paper.

V. Conclusion

We analyzed the feasibility of the electron-beam generation of ExB plasma for airbreathing propulsion. The focus is on power-limited satellites at the altitudes of 100-200 km. The central idea is to use an almost open configuration (a kind of pipe geometry) with a small compression factor (less than 5) in order to minimize the air drag and associated power requirements for the on-board plasma propulsion. This idea is motivated by the previous study of Ref. 8 in which an annular geometry Hall thruster configuration was considered. The concept presented here is based on the cylindrical geometry Hall thruster which has no inner channel parts and therefore, can potentially have lower power requirements due to a smaller air drag than the thruster with the annular geometry. Results of our simplified analysis point to key challenges associated with the use of electron beams for plasma generation at very low pressures relevant to the considered altitudes –1) high beam power requirements, 2) the necessity in effective trapping of beam electrons to maximize their efficient use for ionization, and related to this, 3) beams with considered parameters will likely be subjects to losses due to beam plasma instabilities. To address these challenges, we outlined a number of solutions to consider in the future studies. For example, high power requirements may be relaxed if the electron beams are sourced from another satellite operating at higher altitudes with smaller air drag (also proposed in Ref. 8). It is also shown that at the altitudes higher than 130-140 km, the beam power requirements are smaller than the thruster power required to compensate the air drag. More than that, at the altitudes of higher than 170 km, the required power is a fraction of the power limit which was artificially imposed in our analysis. This limit is linked to the area of the solar panels which, in our study, are limited by the satellite dimensions.

For trapping beam electrons, we consider an ExB configuration similar to cylindrical Hall thrusters and HEMP thrusters. A spread of axial velocity of the electron beam may help to detune beam plasma instability.[29] However, we did not consider here any aspects of the beam trapping and ion acceleration in ExB at relevant low pressures. We also did not consider technical aspects of the magnetic field generation. Finally, no considerations were given to materials

of the thruster components and their potential degradation due to the exposure to chemically reactive environments of the upper atmosphere at the specified altitudes.

Acknowledgments

The authors would like to thank Igor Kaganovich, Mikhail Shneider, Mark Cappelli and Michael Keidar for fruitful discussions. This work was supported by the Air Force Office of Scientific Research.

References

[1] K. Nishiyama, Air breathing ion engine concept, Proc. 54th Int. Astronautical Congr., Bremen, Germany, September 29–October 3, 2003, Paris: Int. Astronaut. Fed., 2003, no. IAC-03-S4-02
[2] S. Barral and L. Walpot "Conceptual design of an air-breathing electric propulsion system", Joint Conf. of 30th Int. Symp. on Space Technology and Science, 34th Int. Electric Propulsion Conf. and 6th Nano-Satellite Symp., Hyogo-Kobe, 2015, IEPC-2015-271
[3] V. Hruby, B. Pote, T. Brogan, K. Hohman, J. Szabo, P. Rostler, "Air breathing electrically powered hall effect thruster", US Patent 6834492 B2 (2002)
[4] L. A. Singh, M. L. R. Walker, "A review of research in low earth orbit propellant collection" Progress in Aerospace Sciences 75 (2015) 15–25
[5] D. DiCara, J. Gonzalez del Amo, A. Santovincenzo et al., RAM electric propulsion for low Earth orbit operation: an ESA study, Proc. 30th Int. Electric Propulsion Conf., Florence, 2007, no. IEPC-2007-162
[6] K. D. Diamant, "A 2-stage Cylindrical Hall Thruster for Airbreathing Electric Propulsion, in: Proceedings of the 46thAIAA/ASME/SAE/ASEE Joint Propulsion Conference &Exhibit, Nashville,TN,2010,AIAA2010-6522 doi:10.2514/ 6.2010-6522
[7] https://www.esa.int/Enabling_Support/Space_Engineering_Technology/World-first_firing_of_air-breathing_electric_thruster
[8] L. Pekker, M. Keidar, "Analysis of airbreathing Hall-effect thrusters, J. Propul. Power28 (2012)1399–1405. http://dx.doi.org/10.2514/1.B34441
[9] Y. Raitses and N. J. Fisch, Parametric Investigations of a Nonconventional Hall Thruster, Phys. Plasmas, 8, 2579 (2001)
[10] S. O. Macheret, M. N. Shneider, and R. C. Murray, "Ionization in strong electric fields and dynamics of nanosecond-pulse plasmas", Phys Plasmas 13, 023502 (2006)
[11] A. T. Powis, P. Porazik, M. Greklek-Mckeon, K Amin, D. Shaw, I. D. Kaganovich, Jay Johnson and Ennio Sanchez "Evolution of a relativistic electron beam for tracing magnetospheric field lines", Front. Astron. Space Sci. 6, 69 (2019)
[12] T. Neubert, B. Gilchrist, S. Wilderman, L. Habash, H.J. Wang, Relativistic electron beam propagation in the Earth's atmosphere: modeling results, Geophys. Res. Lett., 23 (1996)
[13] J. R. Winckler, The application of artificial electron beams to magnetospheric research. Rev. Geophys. 18, 659 (1980)
[14] L R Peterson and A E S Green, "The relation between ionization yields, cross sections and loss functions", J. Phys. B: At. Mol. Phys. 1 1131 (1968)
[15] S. G. Walton et al., Electron Beam Generated Plasmas for Ultra Low T_e Processing, ECS J. Solid State Sci. Technol. 4 N5033 (2015)
[16] F. Marchioni and M. A. Cappelli, Extended channel Hall thruster for air-breathing electric propulsion, J. Appl. Phys. 130, 053306 (2021)
[17] R. R. Hofer, P. Y. Peterson, A. D. Gallimore, R. S. Jankovsky, A High Specific Impulse Two-Stage Hall Thruster with Plasma Lens Focusing, IEPC-01-036, Pasadena, CA, 15-19 October, 2001
[18] L. Dubois et al., ID-HALL, a new double stage Hall thruster design. I. Principle and hybrid model of ID-HALL Phys. Plasmas 25, 093503 (2018); https://doi.org/10.1063/1.5043354
[19] V. L. Bychkov, M. N. Vasilev, and A. P. Zuev, Teplofiz. Vysok. Temp. 32, 323 (1994).
[20] R. F. Fernsler, W. M. Manheimer, R. A. Meger, et al., Production of large-area plasmas by electron Beams", Phys. Plasmas 5, 2137 (1998)
[21] T. Majeed and D. J. Strickland, New Survey of Electron Impact Cross Sections for Photoelectron and Auroral Electron Energy Loss Calculations, Phys. Chem. Ref. Data 26, 335 (1997)
[22] Tsuyohito Ito, Christopher V. Young, and Mark A. Cappelli, Self-organization in planar magnetron microdischarge plasmas Appl. Phys. Lett. 106, 254104 (2015); https://doi.org/10.1063/1.4922898

[23] Y. Raitses, E. Merino, and N. J. Fisch, Cylindrical Hall thrusters with permanent magnets, J. Appl. Phys. 108, 093307 (2010)
[24] J. Simmonds and Y. Raitses, Ion acceleration in a wall-less Hall thruster, J. Appl. Phys. 130, 093302 (2021)
[25] A. Keller et al., "Parametric Study of HEMP-Thruster Downscaling to micro N Thrust Levels," IEEE Trans. Plasma Sci. 43, 45 (2015)
[26] Yu. P. Raizer, Gas Discharge Physics, (Springer-Verlag Berlin Heidelberg 1991)
[27] A. I. Smolyakov et al., Fluid theory and simulations of instabilities, turbulent transport and coherent structures in partially-magnetized plasmas of E x B discharges, Plasma Phys. Control. Fusion 59, 014041 (2017)
[28] Y. Sakawa, C. Joshi, P. K. Kaw, F. F. Chen, and V. K. Jain, Excitation of the modified Simon–Hoh instability in an electron beam produced plasma, Phys. Fluids B 5, 1681 (1993)
[29] R. J. Briggs, Two-stream instabilities, Adv. Plasma Phys. 4, 43 (1971)